Volume 55 | Number 32 | 25 April 2019 | Pages 4591–4740

ChemComm

Chemical Communications

rsc.li/chemcomm

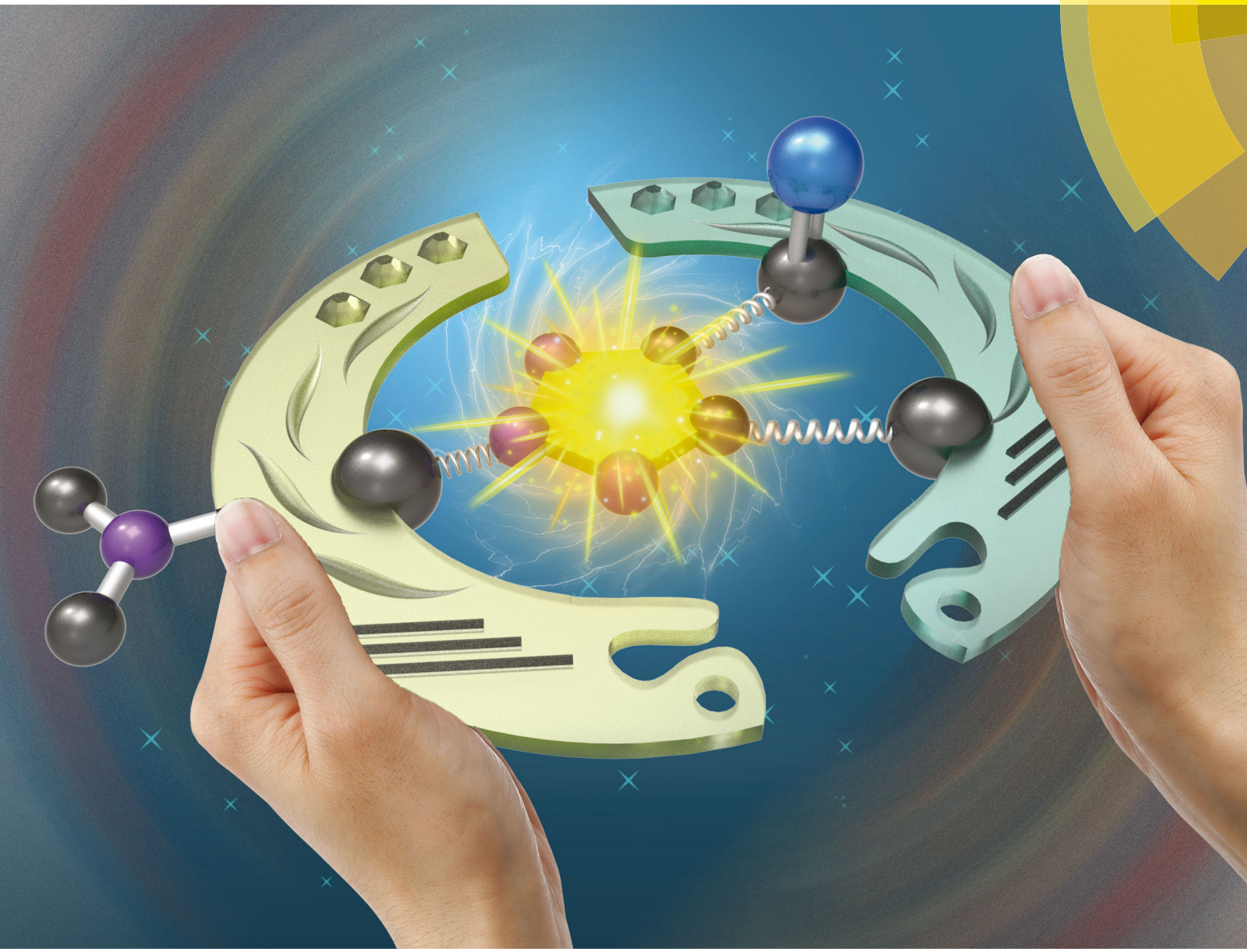

ISSN 1359-7345

ROYAL SOCIETY OF CHEMISTRY | Celebrating IYPT 2019

COMMUNICATION

Xiaodong Shi, Zhiguang Song *et al.*

Rational design and synthesis of yellow-light emitting triazole fluorophores with AIE and mechanochromic properties

ChemComm

COMMUNICATION

View Article Online
View Journal | View Issue

Cite this: *Chem. Commun.*, 2019, **55**, 4603

Received 11th January 2019,
Accepted 7th March 2019

DOI: 10.1039/c9cc00262f

rsc.li/chemcomm

Rational design and synthesis of yellow-light emitting triazole fluorophores with AIE and mechanochromic properties†

Qi Lai,[a] Qing Liu,[a] Kai Zhao,[a] Chuan Shan,[b] Lukasz Wojtas,[b] Qingchuan Zheng,[c] Xiaodong Shi *[ab] and Zhiguang Song*[a]

Previously, we reported that *N*-2-aryl triazoles (NATs) exhibited good fluorescence activity in the UV/blue light range. In an effort to achieve biocompetitive NAT fluorophores with green/yellow emission, a new class of 4-keto-2-(4′-*N*,*N*-diphenyl)-phenyl triazoles were designed and synthesized. Herein, we present our study on these novel fluorophores which demonstrated excellent luminescence emission both in solution (*Φ* up to 96%) and in the solid state (*Φ* up to 43%). Furthermore, these new compounds showed aggregation-induced emission (AIE) properties and reversible mechanochromic luminescence properties, which suggested their potential applications in chemical and materials science.

Fluorescence active small organic molecules are an important class of compounds in chemical,[1] biological[2] and material[3] research. In general, many factors including high luminescence efficiency, high thermal stability, good accessibility and easy modification are assessed for organic phosphor's applications.[4]

In the past decade, our efforts on triazole derivative synthesis[5] have led to the discovery of *N*-2-aryl-1,2,3-triazoles as good fluorescence emission compounds, while the N-1 isomers (1,4-disubstituted-triazole) showed almost no emission.[6] As shown in Scheme 1A, changing different aryl substitutions on both N-2 and C-4 positions can only cause a small emission wavelength shift. Although fluorophores with UV/blue light emission are important for certain applications,[7] those with emission at lower energy (green/yellow/red light region) are preferred for applications in biological systems.[8] Herein, we have devoted much effort to the development of NAT-derivatives with longer emission wavelength. By simultaneously incorporating electron-rich substitutions on the N-2 phenyl position and electron-deficient substitutions on the C-4 position, a series of yellow emitting NAT fluorophores (λ_{em} up to 550 nm) with high quantum yields both in solution and in the solid state were obtained. Moreover, these compounds showed aggregation induced emission (AIE) properties and interesting mechanochromic luminance, suggesting a promising strategy to construct solid fluorophores from simple 1,2,3-triazole derivatives (Scheme 1B).

As a general design principle, extending the conjugation system of fluorophores will lead to a red-shift of the emission wavelength due to the reduced energy gap between its highest occupied molecular orbital (HOMO) and lowest unoccupied molecular orbital (LUMO).[9] Considering that 1,2,3-triazole is a highly electron deficient functional group, incorporation of electron-donating groups (EDG) should cause a red shift of the emission. However, even with strong EDG like *N*,*N*-dimethyl (**1c**), limited red-shift was observed at λ_{em} of 427 nm (Fig. 1A, see detailed syntheses of all compounds and their optical data in the ESI†). Notably, 1,2,3-triazole is a very stable aromatic structure. Thus, it often forms poor conjugation between N-2-aryl triazoles due to energy penalty for breaking aromaticity.

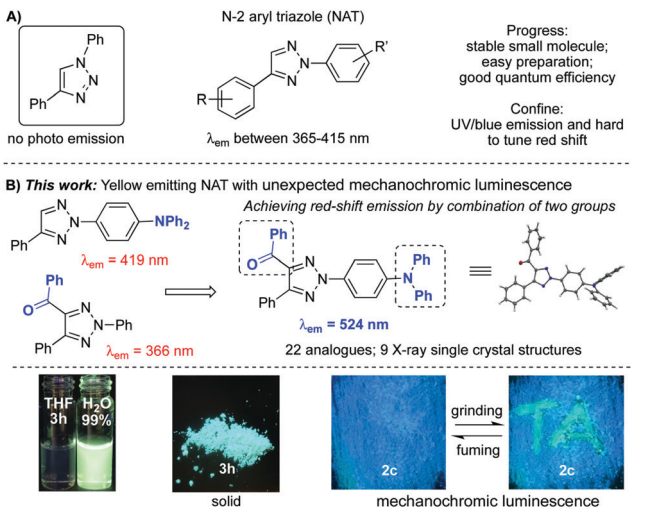

Scheme 1 Developing yellow emitting NAT fluorophores.

[a] *State key Laboratory of Supramolecular Structure and Materials, College of Chemistry, Jilin University, Changchun, Jilin 13002, China. E-mail: szg@jlu.edu.cn*
[b] *University of South Florida, Tampa, FL 33620, USA. E-mail: xmshi@usf.edu*
[c] *International Joint Research Laboratory of Nano-Micro Architecture Chemistry, Institute of Theoretical Chemistry, Jilin University, Changchun 130023, P. R. China*

† Electronic supplementary information (ESI) available. CCDC 1888246–1888254. For ESI and crystallographic data in CIF or other electronic format see DOI: 10.1039/c9cc00262f

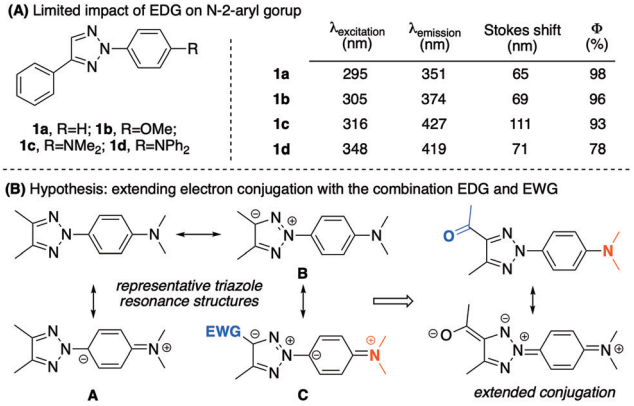

	$\lambda_{excitation}$ (nm)	$\lambda_{emission}$ (nm)	Stokes shift (nm)	Φ (%)
1a	295	351	65	98
1b	305	374	69	96
1c	316	427	111	93
1d	348	419	71	78

Fig. 1 General strategy to achieve a NAT red-shift.

As a result, EDG substituted NAT at best could only form resonance structure **A**, bearing a triazole (TA) stabilized anion, which leads to a limited emission change.

To access extended conjugation, an accessible TA resonance structure **B** is necessary, which requires the overall electron density delocalized from the three adjacent nitrogens to the carbon. With this consideration in mind, we postulated that introducing an electron withdrawing group (EWG) on triazole carbon will help in electron delocalization, favoring the resonance structure **B**. Thus, we proposed that the combination of an EDG on N-2 aryl and an EWG on carbon will build the extended conjugation, giving the desired red-shift NAT as in the case of intermediate **C** (Fig. 1B). To verify this hypothesis, we prepared triazole analogues **2a–2d** with varied EWGs on the C-4 position of triazole. Their PL data are summarized in Fig. 2.

As proposed, introducing an EWG (a cyan or carbonyl group) on the C-4 position resulted in the expected red-shift while maintaining excellent fluorescence emission. Notably, with 4-phenylcarbonyl substitution (**2c**), a very dramatic red-shift (105 nm) was observed. Compared with blue-emitting compounds **2a** and **2b**, the quantum yield for **2c** was lower, which is common for long wavelength emission fluorophores. Density functional theory (DFT) calculations based on single crystal structures were also conducted (Table S13, ESI†). Compared with **2a**/**2b**, **2c** possesses a smaller energy gap (5.83 eV), thus giving a longer wavelength of fluorescence emission. Encouraged by this result, a series of EDG/EWG modified NAT compounds were prepared and their optical properties in THF solution are summarized in Table 1.

First, for all the C-4 phenylcarbonyl substituted triazoles (**3b–3d**), EDGs at N-2 aryl gave rise to an obvious redshift.

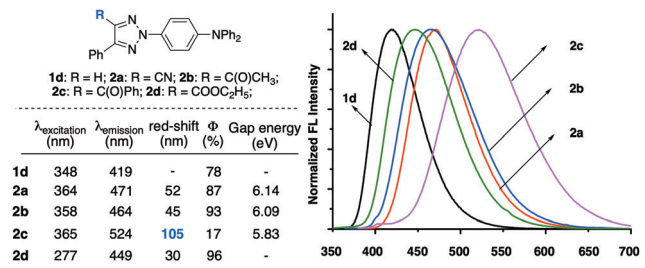

	$\lambda_{excitation}$ (nm)	$\lambda_{emission}$ (nm)	red-shift (nm)	Φ (%)	Gap energy (eV)
1d	348	419	-	78	-
2a	364	471	52	87	6.14
2b	358	464	45	93	6.09
2c	365	524	105	17	5.83
2d	277	449	30	96	-

Fig. 2 Significant red-shift with EDG/EWG substituted TPA-NAT.

Table 1 Optical properties of EDG/EWG modified NAT compounds in THF solution[a]

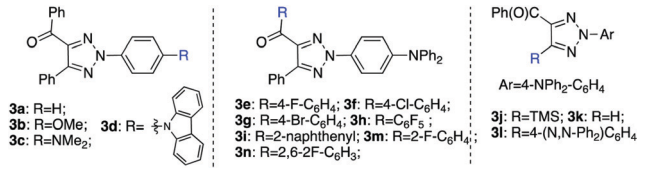

Comp.	λ_{ex} (nm)	λ_{em} (nm)	Life time τ_{avg} (ns)	Φ (%)	Comp.	λ_{ex} (nm)	λ_{em} (nm)	Life time τ_{avg} (ns)	Φ (%)
3a	330	366	3.099	0.37	**3h**	368	470	3.199	0.18
3b	297	377	—	0.62	**3i**	364	537	2.116	18
3c	335	550	6.309	4.1	**3j**	369	533	1.464	52
3d	341	473	1.707	1.3	**3k**	368	530	2.556	36
3e	365	524	3.182	25	**3l**	362	537	1.918	4.3
3f	357	540	2.224	12	**3m**	369	520	3.494	5.7
3g	365	542	1.576	11	**3n**	370	505	1.467	7.8

[a] Fluorescence emission of compounds **3a–3l**. Concentration: 20 μmol L^{-1} in THF.

Interestingly, structurally rigid carbazole substituted NAT **3d** gave rise to a small red-shift, which was likely caused by the poor conjugation between nitrogen and N-2 phenyl due to their steric repulsion. Evaluation of the arylcarbonyl group on the C-4 position confirmed that electron deficient aryl substituents could enhance the overall emission. NATs with 4-F, 4-Br and 4-Cl benzene and naphthenyl substitution all resulted in red-shifts with strong emission. In contrast, the penta-fluoro benzene substituted NAT **3h** gave rise to a small red-shift (λ_{max} = 470 nm) and very low quantum yield in solution. This can be explained by the strong electronic repulsion between F and triazole N, which were confirmed by the crystal structures showing longer distance between F and N (2.908 Å) in **3h** over the H–N distance (2.760 Å) in **3e** (see crystal structures in Fig. S85, ESI†). Similarly, the 2-fluoro phenyl and 2,6-difluoro phenyl substituted NATs **3m** and **3n** also exhibited low fluorescence quantum yield in solution, which further supported the above conclusion.

In addition, different substituents on the C-5 position of triazole were evaluated. Besides phenyl (**2c**), NATs with other functional groups were prepared, including trimethylsilyl (**3j**), hydrogen (**3k**) and electron-donating 4-(*N*,*N*-diphenyl)phenyl (**3l**). Although a red-shift caused by C-5 substitution with either trimethylsilyl or hydrogen was trivial (about 10 nm), the overall emissions remained in the green-yellow light region. Importantly, significant enhancement of emission quantum yields was achieved, which was likely caused by the improved conjugation with less steric hindrance on the C-5 position. Interestingly, incorporation of another EDG on the C-5 position **3l** did not result in efficient emission, which might be ascribed to the lack of effective electronic conjugations. Therefore, by screening NATs of various substitutions, we developed an effective strategy to achieve NAT green/yellow fluorophores *via* tuning the combination of EDGs/EWGs on NATs.

As mentioned above, while electron deficient arylcarbonyl NATs (such as **3f–3g**) generally showed red-shift emissions with high efficiency, it is worth noticing that the pentafluorophenyl substituted NAT **3h** showed poor emission with a quantum yield <1%. To understand the cause of these results, single crystal

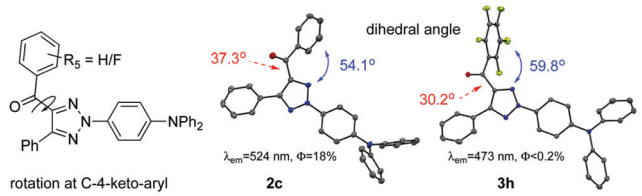

Fig. 3 Crystal structures revealing large dihedral angle.

structures of nine NATs have been successfully obtained (see details in Fig. S78–S86, ESI†). The structures of compounds **2c** and **3h** are shown in Fig. 3. For compound **2c**, the dihedral angle between triazole and carbonyl (C═O) is 37.2° and TA *vs.* Ph is 54.1°, not even close to the coplanar conformation. Moreover, while compounds **2c** and **3h** clearly showed different PL properties in solution, the solid-state X-ray crystals showed a very similar geometry. Their twisted conformation aroused our interest in knowing whether this type of NAT would show different luminescence properties in the solid state and exhibit aggregation-induced emission (AIE).

In 2001, Tang's group first introduced the concept of aggregation-induced emission (AIE) into the community.[10] Since then, a great number of organic molecules have been reported with AIE properties and applied in a wide range of material research and industrial applications.[11] To explore the potential aggregation induced emission of these new types of fluorophores, we first measured their solid-state luminescence properties. The data of some representative compounds are summarized in Table 2 (see detailed data in Fig. S19–S24, ESI†).

Most of the EDG/EWG modified NATs exhibited solid-state emission with different wavelengths. Detailed spectroscopic data along with the CIE 1931 chromaticity diagram are provided in the ESI† (Fig. S25). Importantly, *N*,*N*-diphenyl substitution on the N-2 aryl position is crucial for high solid-state luminance emission (such as **1d**, **2a–2c**, and **3e–3n**) with quantum yields up to 40%.

Table 2 Solid state optical properties of EDG/EWG modified NATs

Comp.	λ_{ex} (nm)	λ_{em} (nm)	Life time τ_{avg} (ns)	Φ (%)	$\Phi_{PL(solid)}/\Phi_{PL(solution)}$
1a	319	362	2.320	7.5	—
1b	275	372	5.426	7.5	—
1c	373	417	7.127	7.7	—
1d	363	423	1.707	30	0.38
2a	275	461	3.182	44	0.51
2b	273	457	2.224	38	0.41
2c	275	457	1.576	21	1.2
2d	274	439	2.000	51	0.53
3a	392	485	—	0.79	—
3b	390	468	2.116	9.1	15
3c	370	504	1.464	5.0	1.2
3d	417	458	—	0.73	—
3e	275	464	1.918	43	1.7
3f	368	513	4.490	13	1.1
3g	360	478	2.166	21	2.0
3h	366	481	4.507	29	161
3i	369	506	4.607	10	0.56
3j	370	502	2.662	18	0.35
3k	368	488	3.696	15	0.42
3l	368	506	2.848	8.5	2.0
3m	370	461	3.128	29	5.1
3n	370	509	5.005	7.4	0.95

To understand this phenomenon, the fluorescence lifetimes (τ) of these NATs were measured both in solution and in the solid state. Based on these data, radiative transition rate constants k_r and nonradiative transition rate constants k_{nr} were calculated. For compound **3h**, in THF solution, transition rate constants are $k_r = 5.627 \times 10^5\ s^{-1}$ and $k_{nr} = 3.128 \times 10^8\ s^{-1}$. In the solid state, these rate constants are $k_r = 6.392 \times 10^7\ s^{-1}$ and $k_{nr} = 1.579 \times 10^8\ s^{-1}$. Thus, it is clear that for compound **3h**, the nonradiative decay is the key factor for the low Φ_{PL} in THF solution.[12] This also leads to the observed 160 time increase of quantum yield in the solid state.

By comparing the fluorescence quantum yields of these compounds in solution and in the solid state, we estimated that many of these new NATs might show effective AIE properties, especially for those compounds with $\Phi_{PL(solid)}/\Phi_{PL(solution)} > 1$, including **2c**, **3b**, **3c**, **3e–3h**, **3l** and **3m**. In fact, the fluorescence intensity of many of these compounds decreased gradually with the increase of water content up to 70% (Fig. 4A). This may be due to the influence of the polarity of solvents on the TICT state.[13] A further increase of the water fraction led to a significant increase of fluorescence intensity, reflecting a typical AIE phenomenon. The titration spectra of compound **3h** are shown in Fig. 4 (see others in Fig. S26–S46, ESI†). Changing the NAT sample measuring temperature from 0 to 50 °C gives a slight blue-shift in most cases, suggesting that the temperature has a small influence on the TICT state (Fig. S13–S18, ESI†). Interestingly, in most of the cases, addition of water (AIE test) gave an unusual hypochromic shift. This may be ascribed to different emission modes of these compounds (*e.g.* local emission *vs.* ICT emission). This was supported by the case of **3c** where two emission bands were observed (Fig. S35, ESI†). One band at short wavelength may have come from the local emission while the other band is related to ICT emission. The observed hypochromic shift may be ascribed to one of these specific emission modes.

During the exploration of NAT solid-state emissions, we found that some of the NATs showed mechanochromic properties. Upon grinding the solid powder, some NATs showed clear red-shift emission. The emission shifts of these compounds are summarized in Table 3.

It is known that grinding could cause the collapse of crystal lattices, converting crystalline materials into amorphous materials.[14] This has been confirmed by powder XRD (Fig. S68–S72, ESI†). Breaking the packing can disrupt the intermolecular interaction, which would force the NATs to adopt a more planar conformation and contribute to the observed mechanochromic luminescence.[15] This emission shift is fully reversible: heating the solid sample to

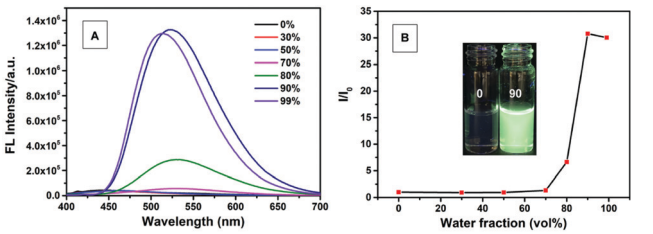

Fig. 4 (A) PL spectra of **3h** (10 μM) in acetone and THF/water mixtures with different water fractions (f_w). (B) Plots of emission intensity of **3h** *versus* the water mixtures.

Table 3 NAT mechanochromic emission[a]

	$\lambda_{em\text{-}solution}$ (nm)	$\lambda_{em\text{-}solid}$ (nm)	λ_{em} grinding (nm)	$\Delta\lambda_{em}$ (nm)
2c	524	457	492	35
3c	550	504	514	10
3e	524	464	487	23
3g	542	478	499	21
3m	520	461	494	33

[a] Here we discuss compounds whose fluorescence emission peaks change more than 10 nm before and after grinding.

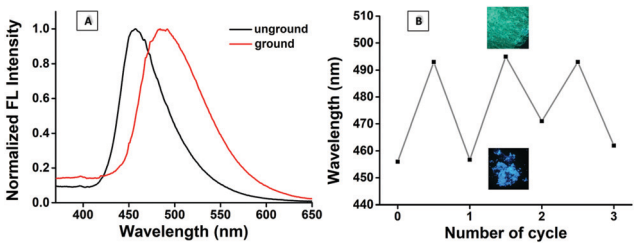

Fig. 5 (A) PL spectra of unground and ground **2c**. (B) Reversible switching of the emission of **2c** through repeated grinding/heating cycles.

170 °C for 1 minute gave the initial emission profile with no change. This process has been repeated multiple times as shown in Fig. 5. Compounds with a twisted conformation (**2c**, **3c**, **3e** and **3g**) demonstrated reasonable emission change after grinding. For **3j** which has a coplanar conformation, emission in the solid state did not change after grinding, suggesting that the twisted conformation between triazole (TA) and 4-arylcarbonyl may be vital to this mechanochromic luminescence. Compounds **3f** and **3h**, both having a twisted conformation in the single crystal form (see Fig. S78–S86, ESI†), did not show mechanochromic properties. This is likely associated with the stronger steric hindrance, making the higher energy barrier adopt the coplanar conformation. The absorption spectra of these NATs under heating and ground conditions were also measured, and no significant changes were observed (Fig. S73–S77, ESI†). Further mechanistic studies on these phenomena are currently undergoing in our lab.

In summary, we reported the successful development of EDG/EWG modified NATs as a new class of organic solid fluorophores with tunable emission from the blue to yellow light region. With the conformations confirmed by single crystal structures, we systematically investigated the relationship between their optical properties and their structures. Notably, the use of a C-4-phenylcarbonyl group and C-5-phenyl in the triazole ring successfully led to a twisted conformation which is crucial for good emission efficiency of NATs in the solid state. What's more, some NATs showed AIE properties and reversible mechanochromic luminescence properties, suggesting promising future for the employment of this strategy in the preparation of new organic solid fluorescent materials.

We are grateful to the NSF (CHE-1665122), NIH (1R01GM120240-01), NSFC (21629201), and Jilin Province (20170307024YY and 20190201080JC) for financial support.

Conflicts of interest

There are no conflicts to declare.

Notes and references

1 (*a*) X. Ai, Y. Chen, Y. Feng and F. Li, *Angew. Chem., Int. Ed.*, 2018, **57**, 2869–2873; (*b*) S. Xu, T. Liu, Y. Mu, Y. F. Wang, Z. Chi, C. C. Lo, S. Liu, Y. Zhang, A. Lien and J. Xu, *Angew. Chem., Int. Ed.*, 2015, **54**, 874–878; (*c*) R. Furue, T. Nishimoto, I. S. Park, J. Lee and T. Yasuda, *Angew. Chem., Int. Ed.*, 2016, **55**, 7171–7175; (*d*) B. Li, J. Lan, D. Wu and J. You, *Angew. Chem., Int. Ed.*, 2015, **54**, 14008–14012; (*e*) H. Wang, P. Chen, Z. Wu, J. Zhao, J. Sun and R. Lu, *Angew. Chem., Int. Ed.*, 2017, **56**, 9463–9467.
2 (*a*) J. Qi, C. Sun, A. Zebibula, H. Zhang, R. T. K. Kwok, X. Zhao, W. Xi, J. W. Y. Lam, J. Qian and B. Z. Tang, *Adv. Mater.*, 2018, **30**, e1706856; (*b*) J. Shi, Y. Li, Q. Li and Z. Li, *ACS Appl. Mater. Interfaces*, 2018, **10**, 12278–12294; (*c*) J. Mei, Y. Huang and H. Tian, *ACS Appl. Mater. Interfaces*, 2018, **10**, 12217–12261; (*d*) J. Qian and B. Z. Tang, *Chem*, 2017, **3**, 56–91.
3 (*a*) L. Yu, Z. Wu, G. Xie, W. Zeng, D. Ma and C. Yang, *Chem. Sci.*, 2018, **9**, 1385–1391; (*b*) M. Gao, H. Su, Y. Lin, X. Ling, S. Li, A. Qin and B. Z. Tang, *Chem. Sci.*, 2017, **8**, 1763–1768; (*c*) T. Yu, D. Ou, Z. Yang, Q. Huang, Z. Mao, J. Chen, Y. Zhang, S. Liu, J. Xu, M. R. Bryce and Z. Chi, *Chem. Sci.*, 2017, **8**, 1163–1168; (*d*) S. Dalapati, E. Jin, M. Addicoat, T. Heine and D. Jiang, *J. Am. Chem. Soc.*, 2016, **138**, 5797–5800.
4 (*a*) J. N. Zhang, H. Kang, N. Li, S. M. Zhou, H. M. Sun, S. W. Yin, N. Zhao and B. Z. Tang, *Chem. Sci.*, 2017, **8**, 577–582; (*b*) S. P. Anthony, *ChemPlusChem*, 2012, **77**, 518–531.
5 (*a*) Y. W. Zhang, X. H. Ye, J. L. Petersen, M. Y. Li and X. D. Shi, *J. Org. Chem.*, 2015, **80**, 3664–3669; (*b*) S. Sengupta, H. F. Duan, W. B. Lu, J. L. Petersen and X. D. Shi, *Org. Lett.*, 2008, **10**, 1493–1496; (*c*) Y. F. Chen, Y. X. Liu, J. L. Petersen and X. D. Shi, *Chem. Commun.*, 2008, 3254–3256; (*d*) Y. X. Liu, W. M. Yan, Y. F. Chen, J. L. Petersen and X. D. Shi, *Org. Lett.*, 2008, **10**, 5389–5392; (*e*) D. W. Wang, X. H. Ye and X. D. Shi, *Org. Lett.*, 2010, **12**, 2088–2091; (*f*) R. Cai, X. H. Ye, Q. Sun, Q. Q. He, Y. He, S. Q. Ma and X. D. Shi, *ACS Catal.*, 2017, **7**, 1087–1092.
6 W. M. Yan, Q. Y. Wang, Q. Lin, M. Y. Li, J. L. Petersen and X. D. Shi, *Chem. – Eur. J.*, 2011, **17**, 5011–5018.
7 D. Dang, Z. Qiu, T. Han, Y. Liu, M. Chen, R. T. K. Kwok, J. W. Y. Lam and B. Z. Tang, *Adv. Funct. Mater.*, 2018, **28**, 1707210.
8 (*a*) Y. Chen, W. Zhang, Y. Cai, R. T. K. Kwok, Y. Hu, J. W. Y. Lam, X. Gu, Z. He, Z. Zhao, X. Zheng, B. Chen, C. Gui and B. Z. Tang, *Chem. Sci.*, 2017, **8**, 2047–2055; (*b*) Z. Li, Y. F. Wang, C. Zeng, L. Hu and X. J. Liang, *Anal. Chem.*, 2018, **90**, 3666–3669.
9 A. Jabłoński, *Nature*, 1933, **131**, 839–840.
10 Y. Hong, J. W. Y. Lam and B. Z. Tang, *Chem. Soc. Rev.*, 2011, **40**, 5361–5388.
11 (*a*) M. H. Lee, A. Sharma, M. J. Chang, J. Lee, S. Son, J. L. Sessler, C. Kang and J. S. Kim, *Chem. Soc. Rev.*, 2018, **47**, 28–52; (*b*) Z. Ruan, Y. Shan, Y. Gong, C. Wang, F. Ye, Y. Qiu, Z. Liang and Z. Li, *J. Mater. Chem. C*, 2018, **6**, 773–780; (*c*) R. T. Kwok, C. W. Leung, J. W. Lam and B. Z. Tang, *Chem. Soc. Rev.*, 2015, **44**, 4228–4238.
12 (*a*) H. T. Feng, Y. X. Yuan, J. B. Xiong, Y. S. Zheng and B. Z. Tang, *Chem. Soc. Rev.*, 2018, **47**, 7452–7476; (*b*) J. B. Xiong, Y. X. Yuan, L. Wang, J. P. Sun, W. G. Qiao, H. C. Zhang, M. Duan, H. Han, S. Zhang and Y. S. Zheng, *Org. Lett.*, 2018, **20**, 373–376.
13 (*a*) M. Jiang, X. Gu, J. W. Y. Lam, Y. Zhang, R. T. K. Kwok, K. S. Wong and B. Z. Tang, *Chem. Sci.*, 2017, **8**, 5440–5446; (*b*) H. Sun, X.-X. Tang, B.-X. Miao, Y. Yang and Z. Ni, *Sens. Actuators, B*, 2018, **267**, 448–456.
14 (*a*) Y. Lei, Y. Zhou, L. Qian, Y. Wang, M. Liu, X. Huang, G. Wu, H. Wu, J. Ding and Y. Cheng, *J. Mater. Chem. C*, 2017, **5**, 5183–5192; (*b*) H. J. Kim, D. R. Whang, J. Gierschner, C. H. Lee and S. Y. Park, *Angew. Chem., Int. Ed.*, 2015, **54**, 4330–4333; (*c*) Y. Sagara, A. Lavrenova, A. Crochet, Y. C. Simon, K. M. Fromm and C. Weder, *Chemistry*, 2016, **22**, 4374–4378; (*d*) Z. Xie, T. Yu, J. Chen, E. Ubba, L. Wang, Z. Mao, T. Su, Y. Zhang, M. P. Aldred and Z. Chi, *Chem. Sci.*, 2018, **9**, 5787–5794.
15 W. Z. Yuan, Y. Tan, Y. Gong, P. Lu, J. W. Lam, X. Y. Shen, C. Feng, H. H. Sung, Y. Lu, I. D. Williams, J. Z. Sun, Y. Zhang and B. Z. Tang, *Adv. Mater.*, 2013, **25**, 2837–2843.

